Mechanistic insights into the co-catalyst effect of Au clusters in Mn-porphyrin-catalyzed olefin oxidation†

Yoshitaka Murakami and Katsuaki Konishi*

Styrene oxidation with iodosylbenzene catalyzed by a Mn-porphyrin/Au-cluster binary system was investigated from several aspects to disclose the mechanism of unique and prominent positive effects of Au clusters. In the catalytic system utilizing a fixed amount of Mn(TPP)Cl (TPP = tetraphenylporphinato) and a varying amount of dodecanethiolate-capped Au cluster (Au:SC12, **1**), the reaction rate was increased sigmoidally with the increase of the charged amount of **1**. From these profiles together with the results of absorption spectral studies, a possible mechanism involving two cluster molecules is proposed. Comparative studies utilizing Mn(TPP)Cl and Mn(TMP)Cl (TMP = tetramesitylporphinato) showed that the latter is superior in terms of the robustness towards oxidative degradation and catalytic activity. Furthermore, at a certain condition, a characteristic induction period was observed only for the reaction with conformationally rigid and sterically hindered Mn(TMP)Cl. Analogous Au clusters protected by non-thiolate ligands such as triphenylphosphine and poly(N-vinyl-2-pyrrolidone) also promoted the catalytic oxidation by Mn(TMP)Cl. Based on these observations, we discuss the critical paths and factors that govern the catalytic activity of the present binary catalyst system.

Introduction

The prominent capability of Au nanoclusters to mediate various oxidative processes has received considerable attention not only based on their fundamental aspects but also in relation to the development of practical oxidation catalysts.[1,2] We have recently provided an example of the unique aspects in the notable positive effects on styrene oxidation with iodosyl-benzene (PhIO) over Mn(TPP)Cl (TPP: tetraphenylporphinato) (Scheme 1).[3,4] This reaction,[5,6] which is rather slow with the Mn catalyst alone under catalytic conditions, proceeded smoothly in the presence of simple dodecanethiolate-capped Au clusters[7] (Au:SC12, average core diameter (d_{av}) = 1.4 or 4.0 nm) to give a high catalytic turnover number (TON). Several control experiments have revealed that the Au cluster itself has no ability to catalyze the styrene oxidation by PhIO but serves as an efficient promoter to accelerate the Mn-porphyrin-mediated reaction.[3] The uniqueness of the Au element constituting the cluster has been demonstrated in comparison with analogous Pd, Ag, and Pt clusters. Absorption spectroscopic studies have indicated that a major role of the Au cluster is to regenerate the active catalytic path involving Mn^{III}/Mn^V from the catalytically ineffective Mn^{IV} species that is inevitably formed in the catalytic cycles (Fig. 1(a)).[8,9]‡

Scheme 1
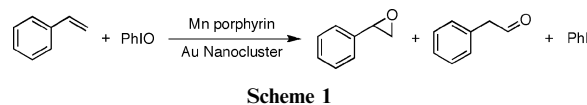
Further studies combined with ^{1}H NMR have implied that two important processes are involved in the reactivation process: (1) the formation of exposed Au surfaces as a result of the irreversible elimination of some dodecyl groups of Au:SC12 by the reaction with PhIO (Fig. 1(b), step 1), and (2) the regeneration of the active forms of the Mn catalyst (Mn^{III}/Mn^V) from the Mn^{IV} species on the exposed Au surface (step 2).[3] We have also suggested that the catalytic cycle turns over Mn porphyrin attached to the Au cluster (step 3), based on the results of spectroscopic investigations and product distribution ratio (epoxide/aldehyde).[3]

In the present paper, we report the results of studies on several factors that affect the activity of the above binary catalyst system, and provide further insights into the role of the Au clusters in the co-catalyst effect. The reaction rates and the oxidation states of the Mn catalyst in styrene oxidation with Mn(TPP)Cl were investigated as a function of the initial amount of Au:SC12 ($d_{av} \sim 1.4$ nm, **1**), from which a plausible catalyst reactivation mechanism involving two cluster molecules is proposed. We also demonstrate that rigid and sterically hindered Mn(TMP)Cl (TMP: tetramesitylporphinato) catalyst is superior in terms of the reaction rates (and also acceleration factors) and stability towards oxidative degradation, and discuss the critical step in the reactivation process based on the difference of Mn(TPP)Cl and Mn(TMP)Cl in the time-course profile. Through studies utilizing analogous Au clusters protected by non-thiolate ligands such as phosphine

Division of Environmental Materials Science, Graduate School of Environmental Science, Hokkaido University, North 10 West 5, Sapporo, 060-0810, Japan. E-mail: konishi@ees.hokudai.ac.jp
† Electronic supplementary information (ESI) available: Absorption spectra of the reaction mixtures under conditions in Fig. 2 and 7. See DOI: 10.1039/b810360g
‡ The true active species under catalytic condition is still elusive (see, ref. 5f). Under our reaction/measurement conditions, the Mn(v)=O species was not detected because of its high reactivity.
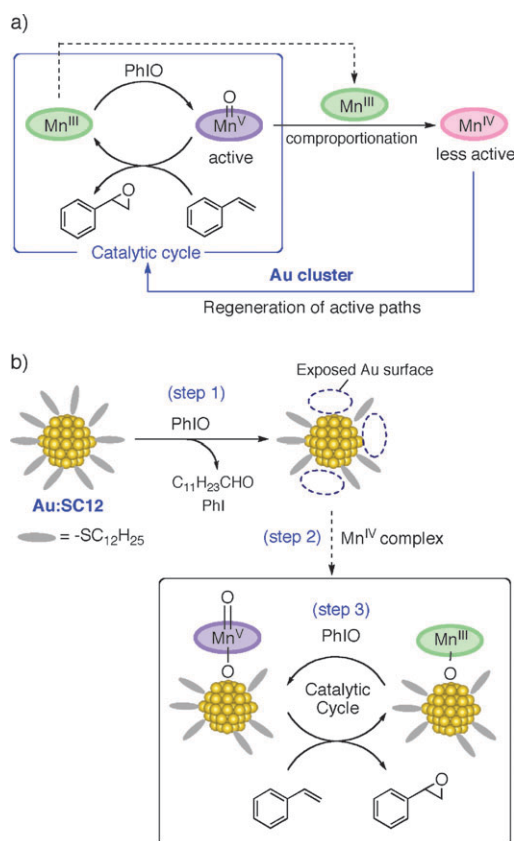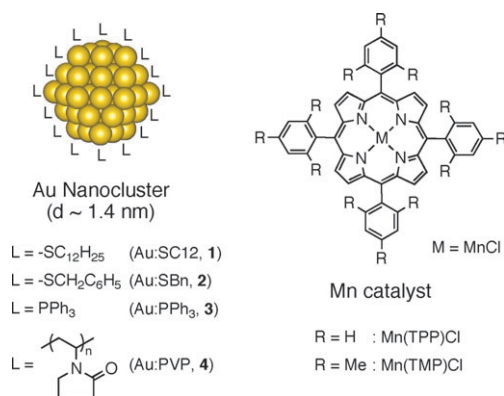
Fig. 1 Outlines of (a) overall catalytic mechanism in the Au cluster/Mn porphyrin system and (b) Mn-catalyst reactivation paths on the Au cluster surface.

(PPh₃) and polymer (PVP), we show that the co-catalyst effect essentially arises from the intrinsic nature of the Au cluster.

Results and discussion

Effects of initial cluster concentration on the catalytic activity

Styrene oxidation with PhIO catalyzed by Mn(TPP)Cl in the presence of a varying amount of **1** was carried out in a similar manner to that reported previously.[3] Thus, a designated amount (0.009–0.18 μmol) of **1** and PhIO (180 μmol) were pretreated in CH₂Cl₂ (2 mL) at 25 °C under Ar, and then the catalytic reaction was started by the addition of Mn(TPP)Cl (0.18 μmol) and styrene (900 μmol). As reported previously,

Table 1 Catalytic Styrene oxidation by **1**/Mn(TPP)Cl system[a]

Entry	$[\mathbf{1}]_0/$ $[Mn(TPP)Cl]_0$	Rate[b] (TON/h)	Relative rate (acceleration factor)	Yield[cd] (%)	Valence of Mn[e]
1	0	17	1.0	17	IV
2	0.05	22	1.3	25	IV
3	0.07	39	2.3	36	IV
4	0.10	44	2.6	40	IV
5	0.15	69	4.1	59	IV
6	0.17	90	5.3	70	IV
7	0.20	117	6.9	83	III/IV
8	0.30	179	10.5	86	III
9	0.50	188	11.1	78[f]	III
10	0.70	195	11.5	71[g]	III
11	1.00	223	13.1	63[g]	III
12	1.50	216	12.7	53[g]	III

[a] $[Mn(TPP)Cl]_0/[styrene]_0/[PhIO]_0 = 0.09/450/90$ mM in CH₂Cl₂ at 25 °C under argon. [b] Estimated from the slope of the linear part in the time course. [c] ([styrene oxide] + [phenylacetaldehyde])/$[PhIO]_0$. [d] After 7 h of reaction unless otherwise noted. [e] From absorption spectrum of the reaction mixture at 2 h. [f] After 4 h. [g] After 3 h.

the reaction in the presence of a sufficient amount of **1** proceeded smoothly to give oxidation products (styrene oxide and phenylacetaldehyde) in high yield (Scheme 1). For example, when the reaction was conducted with 0.054 μmol of **1** (0.3 molar equiv. to Mn(TPP)Cl), the TON ([oxidation products]/$[Mn(TPP)Cl]_0$) after 4 h reached ∼860 (86% yield) (Table 1, entry 8) (Fig. 2, ●), whereas the reaction in the absence of the cluster gave only 10% yield under otherwise identical conditions (entry 1, ×). As revealed from the time courses of the reactions at $[\mathbf{1}]_0/[Mn(TPP)Cl]_0 = 0$, 0.10, 0.15, 0.20, 0.30 and 1.0 (Fig. 2), the acceleration effect drastically depended on the charged amount of **1**. The reaction rates (TON/h) were estimated from the slope of the linear part in the time course (Table 1) and are plotted against $[\mathbf{1}]_0/[Mn(TPP)Cl]_0$ (Fig. 3). As seen in the inset of Fig. 3, the plot showed a sigmoidal feature. Thus, only modest accelerations were observed when the initial ratios were less than 0.1 ($[\mathbf{1}]_0/[Mn(TPP)Cl]_0 = 0.05, 0.07$), but a steep rise of the reaction rates was observed in the region $0.1 \leq [\mathbf{1}]_0/[Mn(TPP)Cl]_0 \leq 0.3$. The rate increase reached saturation at $[\mathbf{1}]_0/[Mn(TPP)Cl]_0 = 0.3$,
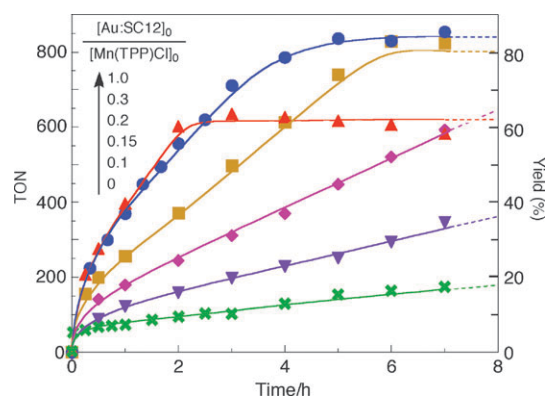

Fig. 2 Time courses of styrene oxidation with PhIO catalyzed by Mn(TPP)Cl in CH₂Cl₂ under argon at 25 °C in the presence of a varying amount of **1** ($[Mn(TPP)Cl]_0/[PhIO]_0/[styrene]_0 = 0.09/90/450$ mM). $[\mathbf{1}]_0/[Mn(TPP)Cl]_0 = 0$ (×), 0.1 (▼), 0.15 (◆), 0.2 (■), 0.3 (●), and 1.0 (▲). TON: ([styrene oxide] + [phenylacetaldehyde])/$[Mn(TPP)Cl]_0$.
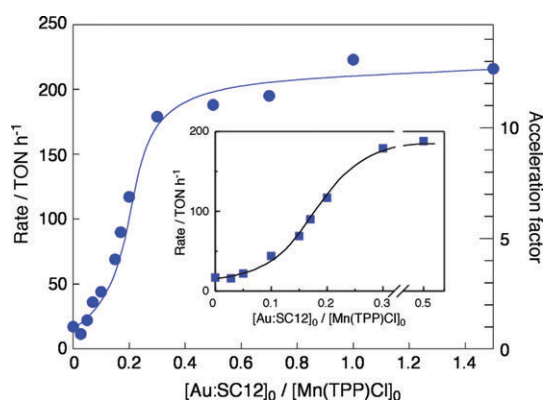
Fig. 3 Correlation of the reaction rate and acceleration factor with the initial cluster/Mn molar ratio $[1]_0/[Mn(TPP)Cl]_0$. The reaction rate was estimated from the linear part in the time course.

where the catalytic reaction was accelerated by a factor of ~ 12 over the background reaction.

Absorption spectra

We also measured absorption spectra of the reaction mixture after 2 h of reaction to investigate the state of the Mn catalyst under reactive conditions. In oxidation reactions catalyzed by Mn porphyrin, Mn^{III} and/or Mn^{IV} complexes are detectable species under conventional reaction/measurement conditions.‡ The Mn^{III} complex ($\lambda_{max} = \sim 480$ nm) is "active," since it can be transformed into the reactive $Mn^V{=}O$ species that is responsible for the substrate oxidation, whereas the Mn^{IV} complex ($\lambda_{max} = \sim 430$ nm) is much inferior in terms of the catalytic activity (Fig. 1(a)). When the reaction was conducted in the absence of the cluster or with a low charge of the cluster ($[1]_0/[Mn(TPP)Cl]_0 \leq 0.17$), less active Mn^{IV} species were predominantly observed in the absorption spectra (430, 525, 666 nm) (Table 1, entries 1–6) (S-Fig. 1a, ESI†). Accordingly, the color of the reaction mixture was orange, which is characteristic of Mn^{IV} porphyrin. As the initial cluster concentration increased, the absorption bands due to Mn^{III} complex appeared and the color of the reaction mixture became greenish. At $[1]_0/[Mn(TPP)Cl]_0 = 0.2$, the mixture showed two Soret bands, indicating the presence of both Mn^{III} and Mn^{IV} species (entry 7) (S-Fig. 1b, ESI†). When the ratio reached 0.3, Mn^{III} porphyrin was observed as the dominant porphyrin species (entries 8–12) (S-Fig. 1c, ESI†). Thus, the rate increase in Fig. 3 is approximately in parallel to the amount of Mn^{III} species present in the reaction system. This observation supports our previous assumption that the major role of the Au cluster is to regenerate the original active path involving Mn^{III}/Mn^V, rather than directly activate the catalyst in the form of the Mn^{IV} complex.[3]

Reactivation mechanism

In our previous paper, we proposed that the reactivation of the catalytically ineffective Mn^{IV} species into the active forms (Mn^{III}/Mn^V) is associated with the redox events on the exposed Au surface.[3] The first reactivation process should occur with the Mn^{IV} species that is initially formed by comproportionation without the involvement of the Au cluster
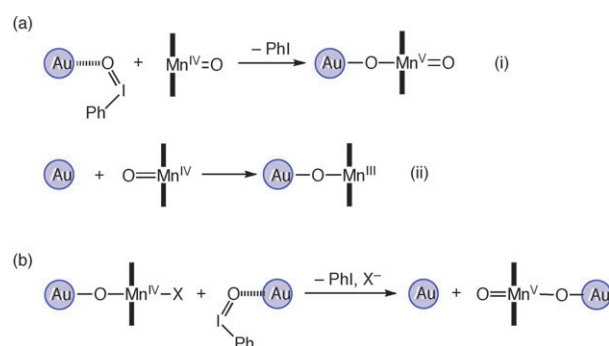
Scheme 2 (a) Possible pathways of the first reactivation process involving free $Mn^{IV}(O)$ porphyrin. (b) A possible reactivation path of the Mn^{IV} species on the Au cluster.

(Fig. 1(a)). Although the axial ligand of the Mn^{IV} species generated under catalytic conditions has not been well identified to date,[7] Newcomb and co-workers recently reported that the substrate-free comproportionation reaction between (TPFPP)Mn^{III}Cl and (TPFPP)$Mn^V{=}O$ (TPFPP: tetrakis-(pentafluorophenyl)porphyrinato) gives (TPFPP)$Mn^{IV}{=}O$.[10] Supposing that such an oxo species was produced in the present catalytic system, two reactivation mechanisms shown in Scheme 2(a) are anticipated: (i) the reaction with the oxidant (PhIO) activated on the Au surface, and (ii) the direct oxidative attack of the oxo group to the Au surface. With either of the mechanisms, the redox process may accompany a linkage formation between the Au surface and the Mn porphyrin. In connection with this, we previously reported definite blue shifts of the absorption bands of Mn^{III} porphyrin in the reaction mixture and distribution ratio of the oxidation products (epoxide/aldehyde) when the catalytic oxidation was conducted at $[1]_0/[Mn(TPP)Cl]_0 = 0.17$.[3] Therefore, it is likely that the Mn catalyst is bound to the Au surface as a consequence of the first reactivation process, and thereafter the subsequent catalytic cycle, which is responsible for the formation of the majority of the oxidation products, occurs over cluster-linked Mn catalyst.

Along with the above mechanism, the promoting effect of the Au cluster appears to arise from its perturbation effect on the reactivity of the linked Mn catalyst to suppress the deactivation (comproportionation). If so, the oxidation rate and the content of the Mn^{III} complex should increase constantly with the increase of $[1]_0$, since the Mn-catalyst once bound to the Au cluster would retain the active form to show high catalytic activity. However, the plot of the reaction rate vs. $[1]_0/[Mn(TPP)Cl]_0$ gave a somewhat peculiar sigmoidal shape (Fig. 3), and the Mn^{IV} species was solely detected in the reaction mixture at the low cluster concentration region (Table 1, entries 1–6) (S-Fig. 1a, ESI†). Accordingly, the Mn-porphyrin catalyst on the Au cluster should also suffer deactivation into the Mn^{IV} species during the catalytic cycle, which must be reactivated to acquire high catalytic activity. At a low feed of the cluster ($[1]_0/[Mn(TPP)Cl]_0 \leq 0.1$), the exposed Au surfaces that serve as the reactivation sites may be already occupied by Mn porphyrins (Fig. 4(a)), so the regeneration process should be inhibited. On the other hand, when a large amount of **1** is initially charged ($[1]_0/[Mn(TPP)Cl]_0 > 0.3$), unoccupied surfaces may be
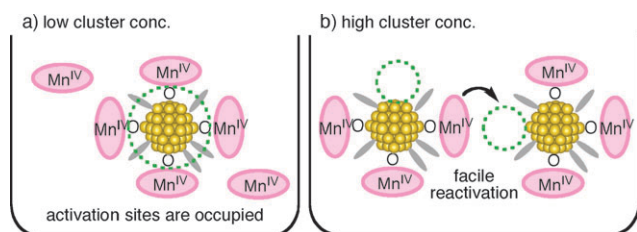
Fig. 4 Schematic illustration of possible molecular events on the Au cluster surface at (a) low cluster concentration and (b) high cluster concentration in the **1**/Mn(TPP)Cl catalyst system.

available to allow effective reactivation of Mn^{IV} species (Fig. 4(b)). Thus, two Au cluster molecules appear to be associated with high catalytic efficiency in the high cluster-concentration condition, where one serves as a scaffold for the Mn porphyrin and the other provides a Mn-catalyst reactivation site. Scheme 2(b) shows a possible reactivation path on the Au cluster. At the present stage it is difficult to provide a clear-cut mechanism because of the ambiguity of the axial ligand of the Mn^{IV} complex. In this respect, more intensive studies including the identification of the Mn-porphyrin/Au-cluster adduct are required to disclose the overall mechanism.

Mn(TPP) *vs.* Mn(TMP): differences in the catalyst lifetime and activity

As shown in Fig. 2 and 3, the rise of the reaction rate upon increasing the initial cluster concentration is almost saturated at $[\mathbf{1}]_0/[Mn(TPP)Cl]_0 = 0.3$. However, when the initial cluster concentration is further increased, the final yield drops. For example, when the reaction was conducted with 1.0 equiv. of **1** (Fig. 2, ▲), the oxidation reaction proceeded with a comparable rate to that observed with 0.3 equiv. of **1** (●) but was almost terminated at 2 h. As a result, the final yield remained at ∼60%, which is evidently lower than that observed with 0.3 equiv. of **1** (∼85%). Metalloporphyrin-based oxidation catalysts occasionally suffer self-degradation by the oxidative attack of highly reactive oxo-metal species,[5] so the loss of the catalytic activity can be attributed to the decomposition of the Mn porphyrin catalyst under the catalytic condition. Actually, the reaction mixture after 7 h showed no absorption bands due to porphyrin species (Fig. 5(a)). Such a degradation was
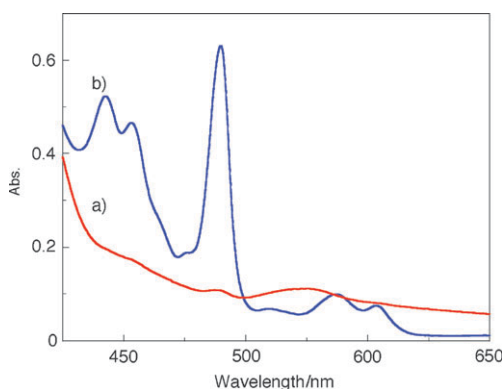

Fig. 5 Absorption spectra in CH_2Cl_2 at 25 °C of the filtered reaction mixtures of (a) **1**/Mn(TPP)Cl and (b) **1**/Mn(TMP)Cl catalyst systems after 7 h of reaction under the conditions given in Fig. 2.
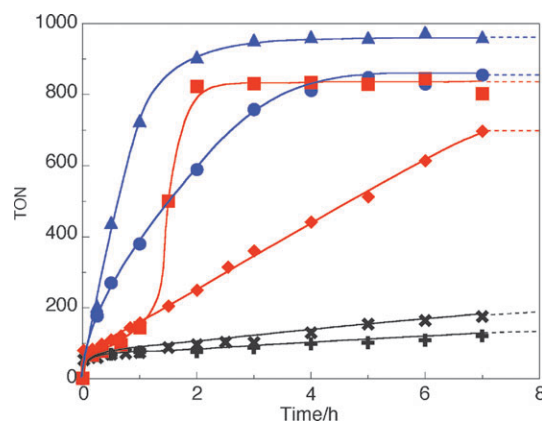

Fig. 6 Time courses of styrene oxidation with PhIO in CH_2Cl_2 under argon at 25 °C catalyzed by **1**/Mn porphyrin ([Mn(TPP)Cl or Mn(TMP)Cl]$_0$/[PhIO]$_0$/[styrene]$_0$ = 0.09/90/450 mM): $[\mathbf{1}]_0$/[Mn(TPP)Cl]$_0$ = 0 (×), 0.17 (◆) and 0.5 (●); $[\mathbf{1}]_0$/[Mn(TMP)Cl]$_0$ = 0 (+), 0.17 (■) and 0.5 (▲).

suppressed at low cluster concentration. When the reaction was conducted at $[\mathbf{1}]_0/[Mn(TPP)Cl]_0 = 0.2$ under otherwise identical conditions, the absorption due to the Mn porphyrin clearly survived.

We also examined the catalytic reaction utilizing Mn(TMP)Cl (TMP: tetramesitylporphinato), which shows excellent stability towards oxidative degradation.[11] Also in the present catalytic system coupled with the Au cluster, Mn(TMP)Cl was much more robust than Mn(TPP)Cl under the catalytic condition. For example, when the reaction was conducted with Mn(TMP)Cl and 0.5 molar equiv. of **1** for 7 h, no significant decrease of the Mn-porphyrin absorptions was found in the reaction mixture (Fig. 5(b)).§ It should also be noted that Mn(TMP)Cl is superior to Mn(TPP)Cl in terms of the reaction rates and acceleration effects by the Au cluster. The reaction catalyzed by Mn(TMP)Cl coupled with 0.5 molar equiv. of **1** (Fig. 6, ▲) proceeded more than three times faster than that with Mn(TPP)Cl (●) (647 and 188 TON/h, respectively). The reaction rate was 76 times larger than that in the cluster-free condition (7.8 TON/h) (×), and the yield reached ∼91% within only 3 h (▲). Thus, Mn(TMP)Cl is an excellent catalyst that shows high reactivity and stability in the presence of the Au cluster.

Another marked difference between Mn(TMP)Cl and Mn(TPP)Cl was found in the time courses when the initial molar equiv. of **1** to the Mn catalyst was decreased to 0.17 (Fig. 6, ◆, ■ and associated lines). The catalytic reaction utilizing Mn(TMP)Cl occurred sluggishly for the initial ∼0.5 h but thereafter proceeded very rapidly (■), whereas such an induction period was hardly observed in the reaction with Mn(TPP)Cl (◆). This difference suggests that the first reactivation process, which occurs with the free $Mn^{IV}(TMP)$ species to allow the linking with the Au surface (Scheme 2(a)), is relatively slow due to the conformational rigidity and sterically hindered metal center of the TMP complex.

§ Similarly to the TPP complex (ref. 3), the TMP complex under the catalytic conditions showed obvious blue shifts (∼11 nm) of the absorption bands around 600 nm (S-Fig. 2, ESI†), suggesting the linking of Mn catalyst with Au cluster.

However, once attached to the Au surface, the Mn^{IV} species generated in the subsequent catalytic cycle may be smoothly reactivated (Fig. 4(b) and Scheme 2(b)) to give high catalytic efficiency, as seen in the fast reaction between 1–2 h in the time course (Fig. 6, ■). Accordingly, the Au cluster scaffold is considered to affect the reactivity of the linked Mn catalyst to assist the reactivation process.

Effects of surface ligands on Au cluster on the catalytic activity

In the experiments described above, we investigated the co-catalyst effect of the Au cluster by using a dodecanethiolate-protected Au cluster (1). We also found that Au clusters of a similar size ($d \sim 1.4$ nm) bearing different protecting ligands cause similar positive effects. For this experiment, we utilized robust Mn(TMP)Cl as the catalyst, and 0.5 molar equiv. of Au cluster was charged. Under this condition, no bleaching of the Mn-porphyrin catalyst (decrease/disappearance of the porphyrin absorptions) was observed at any time during the reaction. Typically, the reaction coupled with a benzylthiolate-protected Au cluster (Au:SBn, 2) proceeded with a comparable rate to that with 1 (Fig. 7(a), ● vs. ▲) to give a TON of ~ 810 after 2 h. When a triphenylphosphine-protected Au cluster (Au:PPh$_3$, 3) was used instead, the time course of the reaction showed an induction period, but thereafter the oxidation reaction occurred very rapidly (■). Based on the above discussion concerning the steric effects on the time course,
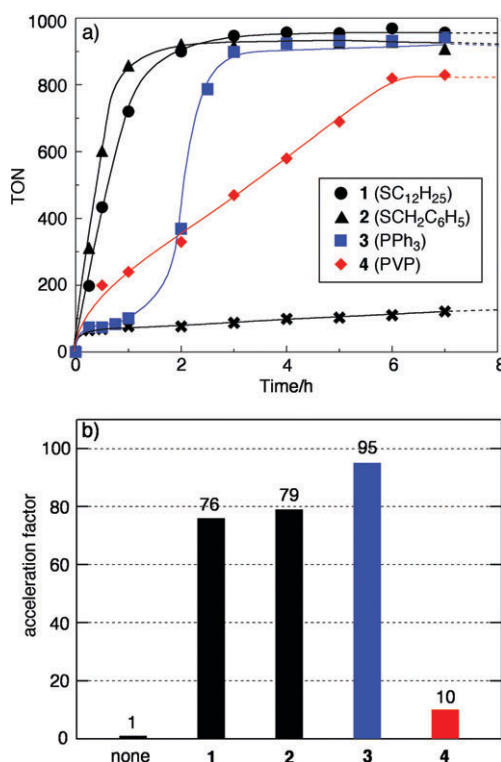
the presence of the induction period suggests that the initial reactivation step involving free Mn^{IV} porphyrin and the Au surface is rather slow due to steric hindrance of the phosphine ligand. A poly(N-vinyl-2-pyrrolidone)-protected Au cluster (Au:PVP, 4) also promoted the reaction, but the rate was significantly slower than those with the thiolate- or phosphine-protected Au clusters (Fig. 7(a) (◆) and (b)). This result agrees well with the reactivation mechanism involving the two clusters illustrated in Fig. 4(b), since the polymer matrix that densely encapsulates the Au core would hamper the bicluster molecular events to lower the reactivation efficiency. Actually, Mn^{IV} porphyrin was observed as the sole porphyrin species in the absorption spectrum of the reaction mixture, whereas active Mn^{III} species was dominant when the other Au clusters protected by low-molecular weight ligands (1–3) were employed (S-Fig. 2, ESI†).§ However, all the Au clusters examined here exhibited definite positive effects on the catalytic reaction. Thus, the reactivation effect essentially originates from the inherent activity of the Au cluster. The high co-catalyst activities of the thiolate- (1, 2) and phosphine- (3) protected Au clusters suggest that the residual ligands provide cavities suitable for the accommodation of the porphyrin catalyst.

Conclusion

In the present study, we investigated the Au-cluster/Mn-porphyrin binary catalyst system in styrene oxidation from several aspects, and we provide mechanistic information on the nature of the unique positive effect of Au clusters. Based on the correlation of the reaction rates with the initially charged amount of Au cluster, we proposed a bicluster mechanism for the facile regeneration of the active Mn-porphyrin species, where one cluster serves as a scaffold and the other serves as a reactivation site for the Mn-catalyst. We have also suggested that the first reactivation process, which occurs with the free Mn^{IV}(TMP) species to allow the linking with the Au surface (Scheme 2(a)), is relatively slow, but, once attached to the cluster, the reactivation of the Mn^{IV} species is facilitated by the linked Au cluster moiety. One of the interesting points that emerged in this study is the unique ability of Au clusters to affect the properties of the linked metalloporphyrin complex. In this respect, studies on the isolation, characterization, and reactivity of the Au-cluster/metalloporphyrin hybrid entity are worthy of further investigations.

Experimental

General

Gas chromatographic (GC) analyses were performed on a Shimadzu Type GC-14B instrument equipped with an FID detector and a RESTEC Stabilwax Rtx-1 dimethylpoly-siloxane capillary column (30.0 m × 0.25 mm × 0.25 mm) using naphthalene as an internal standard. Electronic absorption spectra were measured on a JASCO Type V-550 UV/VIS spectrophotometer by using a quartz cell with a 1-cm path length.

Fig. 7 (a) Time courses of styrene oxidation catalyzed by Mn(TMP)Cl in CH$_2$Cl$_2$ under argon at 25 °C ([Mn(TMP)Cl]$_0$/[PhIO]$_0$/[styrene]$_0$ = 0.09/90/450 mM) in the absence (×) and in the presence of **1** (●), **2** (▲), **3** (■) and **4** (◆) ([Au cluster]$_0$/[Mn(TMP)Cl]$_0$ = 0.5). (b) Relative rates of styrene oxidation catalyzed by Mn(TMP)Cl and Mn(TMP)Cl/Au cluster system. The rate was estimated from the linear part in the time course.

Materials

All solvents including dry CH_2Cl_2 were from Kanto Chemical and were used without further purification. Iodosylbenzene (PhIO), styrene, and poly(N-vinyl-2-pyrrolidone) (PVP-K15, MW $\sim$10000) were purchased from TCI. The chloromanganese(III) complexes of tetraphenylporphyrin [Mn(TPP)Cl] and tetramesitylporphyrin[12] [Mn(TMP)Cl] were synthesized according to previously described procedures.[13] $Au_{55}(PPh_3)_{12}Cl_6$ (**3**, denoted here as Au:PPh$_3$) was prepared by diborane reduction of Au(PPh$_3$)Cl.[14] Au:SC12 (**1**) and Au:SBn (**2**) were synthesized by ligand exchange reaction of **3** with dodecanethiol and benzylthiol, respectively.[3] Au:PVP (**4**) was prepared by NaBH$_4$ reduction of HAuCl$_4$ in the presence of PVP according to a previously described procedure.[15] All clusters have a diameter of $\sim$1.5 nm from TEM and/or SAXS analyses.

Oxidation reactions

Typically, solid PhIO (39.6 mg, 180 μmol) was added to a 20 ml Schlenk tube containing a dry CH_2Cl_2 solution of **1** (0.03 μmol in 1.8 mL) and naphthalene ($\sim$20 mg, internal standard), and the mixture was stirred at 25 °C under argon. After 3 h, a CH_2Cl_2 solution of Mn(TPP)Cl (0.18 μmol/ 0.2 mL) and styrene (105 μL, 900 μmol) were successively added. Aliquots of the reaction mixture were taken at appropriate intervals and subjected to GC analysis to determine the yields of the oxidation products and were then subjected to absorption spectroscopy after centrifugation followed by dilution with CH_2Cl_2. All kinetic runs were conducted in duplicate or triplicate to check the reproducibility.

References

1 For recent reviews, see: (*a*) P. Burks, *Chem. Eng. News*, 2007, September 24, 87; (*b*) T. Ishida and M. Haruta, *Angew. Chem., Int. Ed.*, 2007, **46**, 7154; (*c*) A. S. K. Hashmi and G. J. Hutchings, *Angew. Chem., Int. Ed.*, 2006, **45**, 7896.

2 For selected examples, see: (*a*) M. Haruta, T. Kobayashi, H. Sano and N. Yamada, *Chem. Lett.*, 1987, **16**, 405; (*b*) T. Hayashi, K. Tanaka and M. Haruta, *J. Catal.*, 1998, **178**, 566; (*c*) M. Valden, X. Lai and D. W. Goodman, *Science*, 1998, **281**, 1647; (*d*) M. Comotti, C. D. Pina, R. Matarrese and M. Rossi, *Angew. Chem., Int. Ed.*, 2004, **43**, 5812; (*e*) H. Tsunoyama, H. Sakurai, Y. Negishi and T. Tsukuda, *J. Am. Chem. Soc.*, 2005, **127**, 9374; (*f*) A. Abad, P. Concepción, A. Corma and H. García, *Angew. Chem., Int. Ed.*, 2005, **44**, 4066; (*g*) D. I. Enache, J. K. Edwards, P. Landon, B. Solsona-Espriu, A. F. Carley, A. A. Herzing, M. Watanabe, C. J. Kiely, D. W. Knight and G. J. Hutchings, *Science*, 2006, **311**, 362.

3 Y. Murakami and K. Konishi, *J. Am. Chem. Soc.*, 2007, **129**, 14401.

4 K. Konishi, F. Xu and Y. Murakami, *Chem. Lett.*, 2006, **35**, 476.

5 (*a*) B. Meunier, *Chem. Rev.*, 1992, **92**, 1411; (*b*) C. L. Hill and B. C. Schardt, *J. Am. Chem. Soc.*, 1980, **102**, 6374; (*c*) J. T. Groves, W. J. Kruper and R. C. Haushalter, *J. Am. Chem. Soc.*, 1980, **102**, 6375; (*d*) J. P. Collman, L. Zeng and R. A. Decreau, *Chem. Commun.*, 2003, 2974; (*e*) M. L. Merlau, S. Cho, S. Sun, S. T. Nguyen and J. T. Hupp, *Inorg. Chem.*, 2005, **44**, 5523; (*f*) W. J. Song, M. S. Seo, S. D. George, T. Ohta, R. Song, M. Kang, T. Tosha, T. Kitagawa, E. I. Solomon and W. Nam, *J. Am. Chem. Soc.*, 2007, **129**, 1268.

6 Examples of related Mn complexes: (*a*) Z. Gross, G. Golublov and L. Simkhovich, *Angew. Chem., Int. Ed.*, 2000, **39**, 4045; (*b*) S. H. Wang, B. S. Mandimutsira, R. Todd, B. Ramdhanie, J. P. Fox and D. P. Goldberg, *J. Am. Chem. Soc.*, 2004, **126**, 18.

7 (*a*) *Colloids and Colloid Assemblies*, ed. F. Caruso, Wiley-VCH, Weinheim, 2004; (*b*) M. Brust, J. Fink, D. Bethell, D. J. Schiffrin and C. Kiely, *J. Chem. Soc., Chem. Commun.*, 1995, 1655; R. L. Whetten, M. N. Shafigullin, J. T. Khoury, T. G. Schaaff, I. Vezmar, M. M. Alvarez and A. Wilkinson, *Acc. Chem. Res.*, 1999, **32**, 397; (*c*) A. C. Templeton, W. P. Wuelfing and R. W. Murray, *Acc. Chem. Res.*, 2000, **33**, 27.

8 R. W. Lee, P. C. Nakagaki and T. C. Bruice, *J. Am. Chem. Soc.*, 1989, **111**, 1368.

9 (*a*) J. T. Groves and M. K. Stern, *J. Am. Chem. Soc.*, 1988, **110**, 8628; (*b*) R. D. Arasasingham, G. X. He and T. C. Bruice, *J. Am. Chem. Soc.*, 1989, **115**, 7985.

10 R. Zhang, J. H. Horner and M. Newcomb, *J. Am. Chem. Soc.*, 2005, **127**, 6573.

11 J. P. Collman, J. I. Brauman, P. D. Hampton, H. Tanaka, D. S. Bohle and R. T. Hembre, *J. Am. Chem. Soc.*, 1990, **112**, 7980.

12 J. S. Lindsey and R. W. Wagner, *J. Org. Chem.*, 1989, **54**, 828.

13 K. Konishi. K. Oda, K. Nishida, T. Aida and S. Inoue, *J. Am. Chem. Soc.*, 1992, **114**, 1313.

14 G. Schmid, R. Pfeil, R. Boese, F. Bandermann, S. Meyer, G. H. M. Calis and J. W. A. van der Velden, *Chem. Ber.*, 1981, **114**, 3634.

15 H. Tsunoyama, Y. Negishi and T. Tsukuda, *J. Am. Chem. Soc.*, 2006, **128**, 6036.